Available online at www.sciencedirect.com
SCIENCE DIRECT®
Composites Science and Technology 63 (2003) 1599–1605
COMPOSITES SCIENCE AND TECHNOLOGY
www.elsevier.com/locate/compscitech

A molecular dynamics simulation study of nanoparticle interactions in a model polymer-nanoparticle composite

James S. Smith[a], Dmitry Bedrov[a], Grant D. Smith[a,b,*]

[a]*Department of Materials Science and Engineering, University of Utah, 122 S. Central Campus Drive, Rm. 304, Salt Lake City, UT 84112, USA*
[b]*Department of Chemical and Fuels Engineering, University of Utah, 122 S. Central Campus Drive, Rm. 304, Salt Lake City, UT 84112, USA*

Received 4 September 2002; received in revised form 8 November 2002; accepted 15 December 2002

Abstract

Molecular dynamics (MD) simulations were performed on a model polymer–nanoparticle composite (PNPC) consisting of spherical nanoparticles in a bead-spring polymer melt. The polymer-mediated effective interaction (potential of mean force) between nanoparticles was determined as a function of polymer molecular weight and strength of the polymer–nanoparticle interaction. For all polymer–nanoparticle interactions and polymer molecular weights investigated the range of the matrix-induced interaction was greater than the direct nanoparticle–nanoparticle interaction employed in the simulations. When the polymer–nanoparticle interactions were relatively weak the polymer matrix promoted nanoparticle aggregation, an effect that increased with polymer molecular weight. Increasingly attractive nanoparticle–polymer interactions led to strong adsorption of the polymer chains on the surface of the nanoparticles and promoted dispersion of the nanoparticles. For PNPCs with strongly adsorbed chains the matrix-induced interaction between nanoparticles reflected the structure (layering) imposed on the melt by the nanoparticle surface and was independent of polymer molecular weight. The nanoparticle second virial coefficient obtained from the potential of mean force was utilized as an indicator of dispersion or aggregation of the particles in the PNPC, and was found to be in qualitative agreement with the aggregation properties obtained from simulations of selected PNPCs with multiple nanoparticles.

Keywords: A. Nanostructures; A. Particle-reinforced composites; A. Polymer-matrix composites (PMCs); B. Modeling; C. Computational simulation

1. Introduction

Particles are important additives for altering and enhancing the properties of polymers [1]. A well-known example is the addition of carbon black to rubbers that is responsible for increased strength and durability [2,3]. Because of their very high surface area to volume ratio, the effect of nanoscopic particles (nanoparticles) on the properties of a polymer matrix and the resulting properties of the polymer–nanoparticle composite, or PNPC, can be much more dramatic than is observed in conventional polymer–particle composites. Such PNPCs exhibit promising properties for a wide variety of applications [4–8]. The properties of PNPCs are strongly influenced by nanoparticle size and filler fraction, nanoparticle shape, nanoparticle distribution, polymer molecular weight and the nature of the interactions between the nanoparticle and polymer matrix. There is a great need for insight that can be provided by theory and simulation regarding factors controlling the dispersion of nanoparticles and the properties of the PNPCs as a function of these parameters.

The application of theory and simulation methods to PNPCs is much less mature than in the related field of colloidal suspensions. Theoretical efforts that have been successful for colloid-polymer solutions (e.g., [9–16]) have not been fully extended to the dense polymer melts typical of a PNPC. Furthermore, until quite recently [15] theoretical studies of colloid-polymer solutions have dealt almost exclusively with cases where the radius of the colloidal particle is large compared to the radius of gyration of the polymer. The number of

* Corresponding author. Fax: +1-801-581-4816.
E-mail address: gsmith2@gibbon.msu.utah.edu (G.D. Smith).

0266-3538/03/$ - see front matter © 2003 Published by Elsevier Ltd.
doi:10.1016/S0266-3538(03)00061-7

molecular simulation studies [17–19] that have been performed on PNPCs in order to gain insight in their structure and dynamics is also quite limited. These simulations revealed that the presence of nanoparticles as well as the strength of nanoparticle–polymer interactions strongly influence the dynamics, viscosity, and dynamic shear modulus of the polymer matrix and PNPC. Balazs et al. have shown in a series of lattice Monte Carlo and self-consistent field simulations [20–24] of diblock copolymer/nanoparticle mixtures that nanoparticle-polymer interactions strongly influence the dispersion of nanoparticles. In the present work molecular dynamics (MD) simulations have been employed to examine the polymer-induced interactions between nanoparticles in a dense polymer matrix as a function of polymer molecular weight and the strength of the nanoparticle-polymer interaction, and to correlate polymer matrix effects with the dispersion of nanoparticles in a model PNPC. Here we concentrate on the regime where the radius of the particle, the radius of gyration of the polymer and the statistical segment length of the polymer are comparable which is particularly difficult to address theoretically [15,16].

2. System description and simulation methodology

2.1. Coarse-grained polymer–nanoparticle composites

MD simulations as described below were performed on PNPCs consisting of two or five nanoparticles in a melt of 400, 800 and 1600 bead-necklace chains of length 20, 10, or 5 beads, respectively. The systems with two nanoparticles were utilized to determine the potential of mean force between the nanoparticles which was subsequently used to calculate second virial coefficient. These results were qualitatively compared with the dispersion/aggregation behavior of nanoparticles in the five nanoparticle systems. The polymer chains were modeled as bead necklace chains [25,26] with bead diameters of σ, defining the reference length scale. Each bead corresponds to 4–7 monomer units in a real, flexible polymer chain. Bond lengths were constrained to σ using the standard shake algorithm [27]. The polymer beads interacted with other polymer beads by Lennard-Jones interactions with a well depth of one ($\varepsilon_{pp}=1$), defining the energy scale for the simulations. The radius of gyration, R_g, of the bead necklace chains in a pure melt were 2.24σ (20 bead chains), 1.50σ (10 bead chains), and 0.98σ (5 bead chains).

The nanoparticles were modeled as spheres of Lennard–Jones radius $R_n=2.5\sigma$. The interactions between nanoparticles, U_{nn}, and between polymer beads and nanoparticles, U_{np}, were modeled using modified Lennard–Jones functions which account for the excluded volume of the beads and particles by offsetting the interaction range by R_{EV}:

$$U_{nn}(r)=\infty \qquad r\leqslant R_{EV}=4.0\sigma$$

$$U_{nn}(r)=4\varepsilon_{nn}\left[\left(\frac{\sigma}{r-R_{EV}}\right)^{12}-\left(\frac{\sigma}{r-R_{EV}}\right)^{6}\right] \qquad r>R_{EV}=4.0\sigma \tag{1a}$$

$$U_{np}(r)=\infty \qquad r\leqslant R_{EV}=2.0\sigma$$

$$U_{np}(r)=4\varepsilon_{np}\left[\left(\frac{\sigma}{r-R_{EV}}\right)^{12}-\left(\frac{\sigma}{r-R_{EV}}\right)^{6}\right] \qquad r>R_{EV}=2.0\sigma \tag{1b}$$

where r is the separation distance between two interacting sites and the choice of interaction parameters ε_{nn} and ε_{np} is described below. All interactions in the system were truncated and shifted so that the energy and force are zero at the separation $r=R_{EV}+2.5\sigma$ ($R_{EV}=0.0$ for polymer bead–polymer bead interactions).

In our simulations the interparticle interaction parameter ε_{nn} was fixed so that the excess nanoparticle second virial coefficient, B_2^{EX}, is zero in the absence of polymer. The excess second virial coefficient is the second virial coefficient for the nanoparticle gas less B_2^{HS}, the second virial coefficient for hard spheres of diameter $R_{EV}=4.0\sigma$ and was calculated using the relation [28]:

$$B_2^{EX}=-\tfrac{1}{2}\int_{R_{EV}}^{\infty}[\exp(-\beta U_{nn}(r))-1]4\pi r^2\mathrm{d}r \tag{2}$$

A value of $B_2^{EX}=0$ was obtained for $\varepsilon_{nn}=1.412$ which then was used in all simulations to represent nanoparticle–nanoparticle interactions. For each system we have performed simulations for nanoparticle-polymer interactions $\varepsilon_{np}=1.0$, 2.0 and 3.0.

2.2. Simulation methodology

MD simulations for the PNPCs described above were carried out using the simulation package *Lucretius* [29]. All simulations were carried out in a periodic cubic cell at temperature $T^*=1.33$ in units of ε_{pp}/k_B where k_B is the Boltzmann constant. Initially the systems were simulated in the NPT ensemble using the extended ensemble method [30] for at least 20 polymer chain relaxation times (Rouse times) at pressure $P=0$ yielding equilibrium densities $\rho^*=0.70$, 0.68, and 0.63 for 20, 10, and 5 bead chains, respectively. The PNPCs were subsequently equilibrated in the NVT ensemble for at least 100 polymer relaxation times. Production runs of $t^*=71.5\times10^3$ were carried out in the NVT ensemble

using a time step $\delta t^* = 5.5\times10^{-3}$ with time reported in reduced units defined as $t^* = (\varepsilon_{pp}/m\sigma^2)^{1/2}t$. This was significantly longer than the polymer Rouse times which were 154, 35 and 8 for the 20, 10 and 5 bead polymer chains, respectively. A similar procedure was employed for all simulations conducted including umbrella sampling described in the next section.

2.3. Umbrella sampling and multiple histogram technique

The potential of mean force $V(r)$ as a function of nanoparticle separation r can be calculated directly from simulations of the PNPCs containing two nanoparticles and is given by

$$V(r) = -k_B T \ln p_o(r) \tag{3}$$

where $p_o(r)$ is the probability of finding the nanoparticles separated by distance r during a simulation. Unfortunately, $p_o(r)$ can be quite small for separations of interest, precluding sufficiently accurate sampling during a standard MD simulation run. Hence, the umbrella sampling technique [31] was used to obtain $V(r)$. Here, in addition to nanoparticle–nanoparticle and polymer bead–nanoparticle interactions described above in Eqs. (1a) and (1b), a biasing or window potential $U^*(r)$ between the particles was used to force the particles to sample the full range of interparticle distances available in the simulation box. The biasing potential was a simple harmonic spring, or

$$U_i^*(r) = \tfrac{1}{2}k(r - R_i)^2 \tag{4}$$

Such a biasing potential for the ith window creates an umbrella-shaped distribution of interparticle separations around the predefined distance R_i. For each PNPC five umbrella sampling simulations were run with $R_i = 5.0\sigma$, 6.0σ, 7.0σ, 8.0σ and 9.0σ and $k = 4.0$. This provided a set of interparticle distance histograms with sufficient overlap between the neighboring distributions. The self-consistent histogram method [32,33] was used in order to obtain the unbiased probability distribution of interparticle distances $p_o(r)$ from the umbrella sampling histograms.

3. Results

3.1. Role of the polymer–nanoparticle interaction potential on effective nanoparticle interactions

The potential of mean force $V(r)$ obtained from MD simulations as a function of nanoparticle separation is shown for $\varepsilon_{np} = 1.0$, 2.0 and 3.0 for chain lengths $n = 20$, 10 and 5 in Fig. 1a, b and c, respectively. The influence of the polymer matrix on the nanoparticle potential of mean force can be determined by subtracting the bare nanoparticle–nanoparticle interaction [Eq. (1a)], shown in Fig. 2a, from $V(r)$, i.e., $V_{matrix}(r) = V(r) - U_{nn}(r)$, where $V_{matrix}(r)$ is the effective nanoparticle–nanoparticle potential due to the polymer matrix. The resulting $V_{matrix}(r)$ is shown in Fig. 2b, c and d for $\varepsilon_{np} = 1.0$, 2.0 and 3.0, respectively.

For the weakest polymer–nanoparticle interaction strength investigated, i.e., $\varepsilon_{np} = 1.0$, a distinct minimum in $V(r)$ at a separation 5.0σ is observed. This corresponds to a strong probability of finding the nanoparticles of Lennard–Jones diameter 5.0σ dimerized, as illustrated in Fig. 3a. Examination of $V_{matrix}(r)$ for $\varepsilon_{np} = 1.0$ (Fig. 2b) reveals that the tendency for nanoparticle dimerization (aggregation) is not driven primarily by the bare nanoparticle-nanoparticle interaction but rather by the polymer matrix, which strongly prefers configurations with close nanoparticle–nanoparticle contact. Figs. 1 and 2 reveal that as the polymer–nanoparticle interactions become increasingly favorable ($\varepsilon_{np} = 2.0$ and $\varepsilon_{np} = 3.0$) the effective nanoparticle–

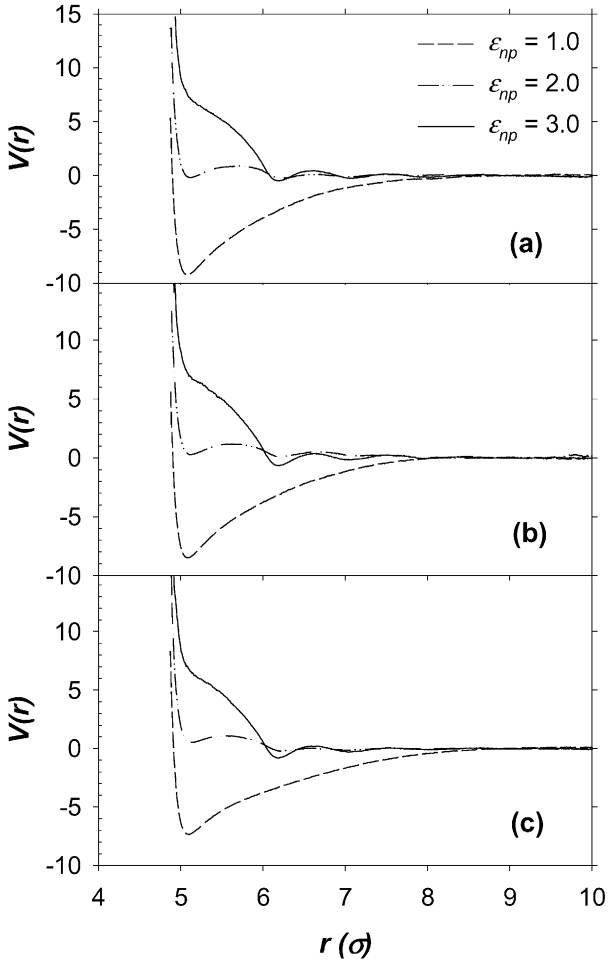

Fig. 1. Potential of mean force, $V(r)$, for (a) 20 bead, (b) 10 bead and (c) five bead chains.

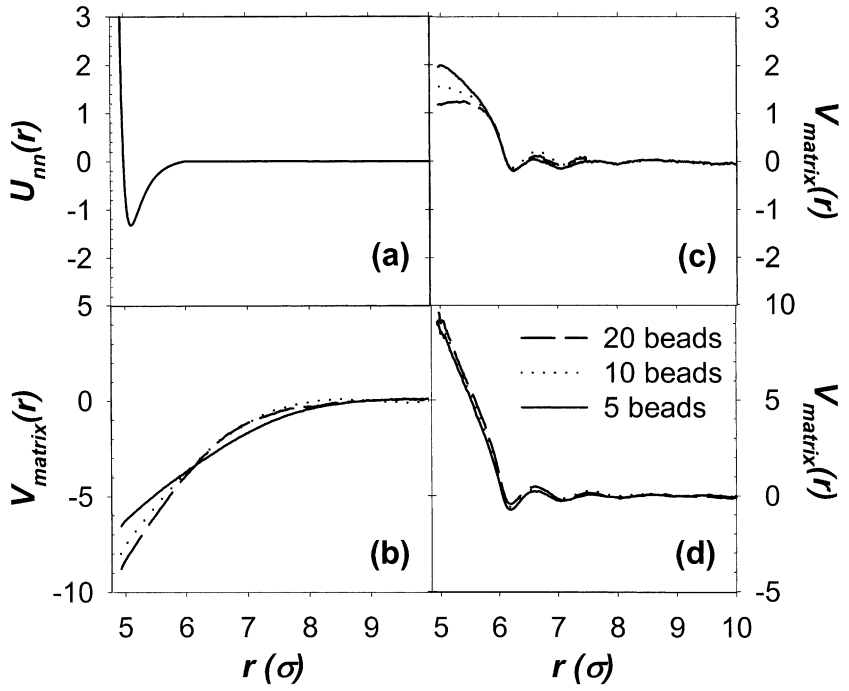

Fig. 2. Comparison of effective interparticle potential due to the matrix $V_{\text{matrix}}(r)$, calculated by subtracting the bare interparticle potential $U_{\text{nn}}(r)$ shown in (a) from $V(r)$, for different polymer molecular weights with (b) $\varepsilon_{\text{np}}=1.0$, (c) $\varepsilon_{\text{np}}=2.0$ and (d) $\varepsilon_{\text{np}}=3.0$.

nanoparticle interaction $V(r)$ becomes increasingly less favorable. The minimum at 5.0σ begins to disappear indicating that it is no longer favorable for the nanoparticles to strongly dimerize. New, much weaker, minimums in $V(r)$ and $V_{\text{matrix}}(r)$ appear at 6.0σ and 7.0σ. These features indicate an increased likelihood to find one or two polymer layers between the nanoparticles as the chains begin to adsorb onto the surface of the nanoparticle due to the large ε_{np} values, as illustrated schematically in Figs. 3b and c.

Longer-range structure in $V(r)$ and $V_{\text{matrix}}(r)$ with a spacing of σ can also be seen for $\varepsilon_{\text{np}}=2.0$ and $\varepsilon_{\text{np}}=3.0$, reflecting the structure, or layering, known to be imposed on the matrix by strongly adsorbing interfaces [17,18]. Such layering is not observed at interfaces with weaker polymer-surface interactions [18]. Interface-induced structure in the polymer matrix is clearly reflected in the average density of polymer beads in a cylinder of radius 1.0σ centered on the line of closest

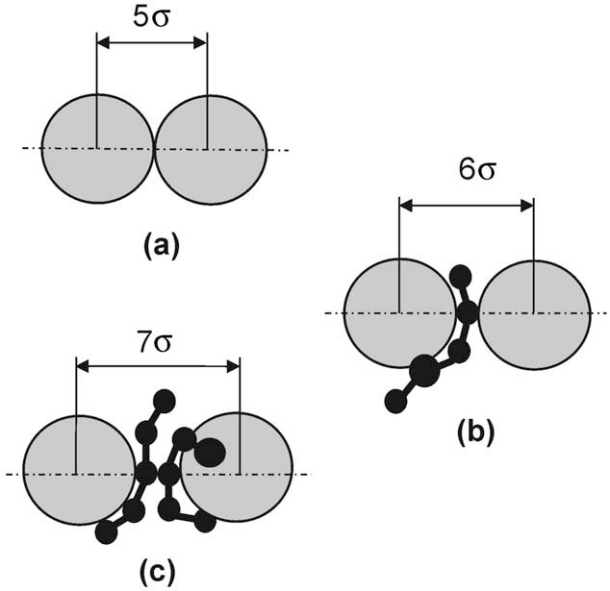

Fig. 3. Schematic illustration of nanoparticle–nanoparticle contact for three different separations: (a) 5.0σ, (b) 6.0σ and (c) 7.0σ. Cases (b) and (c) are valid only for strongly adsorbing polymer–nanoparticle interactions ($\varepsilon_{\text{np}}=2.0$ and 3.0).

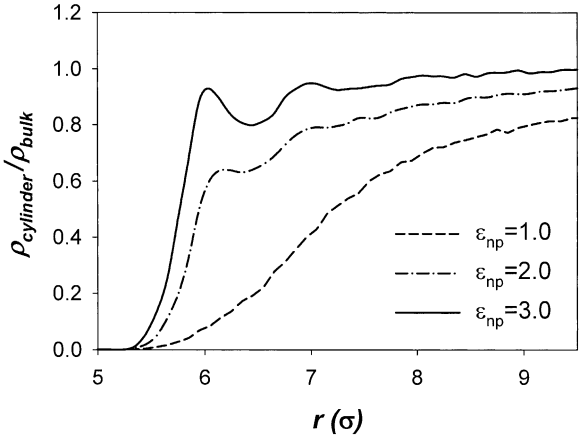

Fig. 4. Ratio of density of polymer beads in the cylinder of radius 1.0σ centered on the line of closest approach between nanoparticles to the bulk density as a function of nanoparticle separation for different strength of the polymer–nanoparticles interation for 20 bead chains.

approach between nanoparticles as a function of nanoparticle separation, shown in Fig. 4. For the weakest interaction energy, $\varepsilon_{np} = 1.0$, the polymer bead density between particles decays monotonically from near bulk density at large separation to zero at $r < 6.0\sigma$ where it is no longer possible to insert a polymer bead between the surfaces. This corresponds well to the smooth drop in the potential of mean force for the same range shown in Fig. 2b, and is consistent with the absence of surface-induced structure for melts with weak polymer–surface interactions [17,18]. For more attractive nanoparticle–polymer interactions the bead density manifests features (minima and maxima) with spacing equal to the monomer diameter, σ, consistent with structure seen in the potential of mean force (Fig. 2c and d) for these systems, and consistent with surface-induced layering [17,18]. These features are exhibited until a nanoparticle spacing of 6.0σ below which the polymer bead density again quickly drops to zero.

3.2. Nanoparticle second virial coefficient

The nanoparticle second virial coefficient, B_2, can be determined from the potential of mean force $V(r)$ between nanoparticles using the relationship:

$$B_2 = -\tfrac{1}{2}\int_0^\infty [\exp(-\beta V(r)) - 1] 4\pi r^2 \mathrm{d}r \quad (5)$$

B_2 serves as a measure of the perturbation from ideality (ideal gas) of the nanoparticles due to bare nanoparticle interactions and effective interactions induced by the matrix. While knowledge of the second virial coefficient alone is usually insufficient to allow prediction of phase behavior, it is a good indicator of the tendency of particles to aggregate or disperse within a solution. As many body effects (manifested in higher-order virial coefficients) typically result in a net repulsive contribution to the particle–particle interaction in polymer matrices [14], a positive value of B_2 essentially precludes phase separation. Conversely, a negative value for B_2 is indicative of a tendency for the nanoparticles and polymer to phase separate. Fig. 5 shows B_2 as a function of ε_{np} for each polymer molecular weight investigated. The PNPCs with the weakest ε_{np} exhibit large negative values of B_2 consistent with the strong tendency toward dimerization observed in the potential of mean force. As ε_{np} increases B_2 becomes rapidly less negative and for $\varepsilon_{np} = 2.0$ and 3.0 the B_2 is positive, favoring the random dispersion of nanoparticles in the polymer melt for all molecular weights investigated.

3.3. Simulations of PNPCs with multiple nanoparticles

Simulations of five nanoparticles in a 20 bead polymer melt were performed with the same interactions as in the umbrella sampling simulations with two nanoparticles

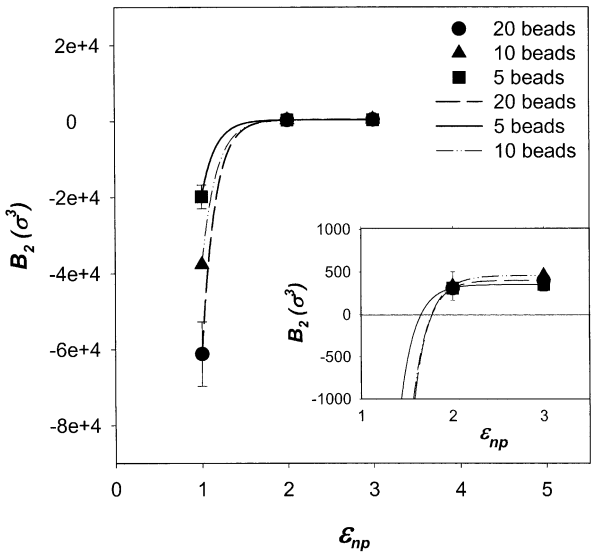

Fig. 5. Second virial coefficient behavior as a function of ε_{np} for different polymer molecular weights. Inset shows magnified scale for the values of $\varepsilon_{np} = 2.0$ and 3.0. B_2 is calculated from the simulated potential of mean force, $V(r)$, between two nanoparticles (see text). Lines serve to guide the eye. Error bars were determined from statistical variance between individual simulation runs.

discussed above. The simulations of PNPCs containing five nanoparticles will not allow us to map out the phase diagram of the PNPC due to finite size effects. However, they are useful in helping determine if the nanoparticles have a tendency to aggregate which is a necessary condition for formation of a nanoparticle rich phase. Simulations with $\varepsilon_{np} = 1.0$ showed a strong tendency for the nanoparticles to aggregate in a roughly spherical compact cluster as illustrated by the sharp peak in the nanoparticle-nanoparticle radial distribution function, $g_{nn}(r)$, in Fig. 6. As ε_{np} increases the nanoparticles disperse in the matrix as illustrated by the disappearance of the strong first peak in $g_{nn}(r)$ and the flat distribution of interparticle separation ($g_{nn}(r) \approx 1.0$) in Fig. 6. This

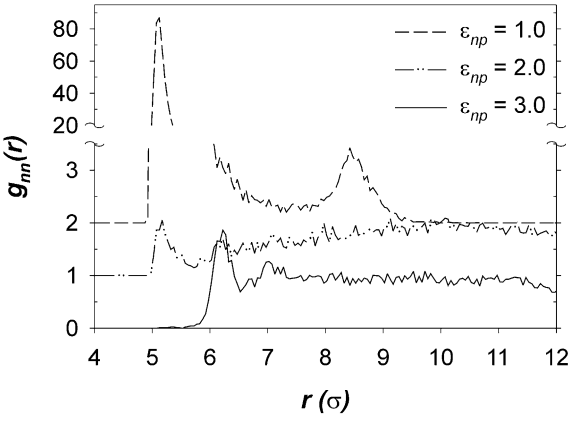

Fig. 6. The nanoparticle–nanoparticle radial distribution functions from MD simulations of five nanoparticles in a 20 bead polymer melt for different values of ε_{np}. Data are offset vertically by 2.0 and 1.0 for $\varepsilon_{np} = 1.0$ and $\varepsilon_{np} = 2.0$, respectively.

dependence of nanoparticle aggregation on ε_{np} is in qualitative agreement with the potential of mean force and second virial coefficients obtained from the two nanoparticle PNPC simulations, indicating that the second virial coefficient of nanoparticles in the polymer matrix can provide a useful indication of nanoparticle aggregation behavior.

3.4. Effect of polymer molecular weight on effective nanoparticle interactions

Fig. 2b reveals that for aggregating nanoparticles ($\varepsilon_{np} = 1$), the influence of the polymer matrix on the effective nanoparticle-nanoparticle interaction appears to decrease with decreasing polymer molecular weight. With increasing strength of the polymer-nanoparticle interaction, the influence of chain length on $V_{matrix}(r)$ decreases dramatically, as revealed in Figs. 2c and d. We believe the molecular weight dependence of $V_{matrix}(r)$ observed for $\varepsilon_{np} = 1.0$ and $\varepsilon_{np} = 2.0$ is a consequence of enrichment of chain ends at the particle surface due to interfacial restrictions on polymer configeration entropy [34]. Short chains have a higher proportion of chain ends and hence are more effective in wetting particle surfaces than long chains. For stronger polymer–nanoparticle interactions (e.g., $\varepsilon_{np} = 3.0$), the attraction appears to be strong enough to overcome configerational entropy effects and hence end effects become insignificant. To date, we have not resolved individually the entropic and energetic contributions to $V_{matrix}(r)$ and their dependence on molecular weight and the strength of the nanoparticle-polymer interaction.

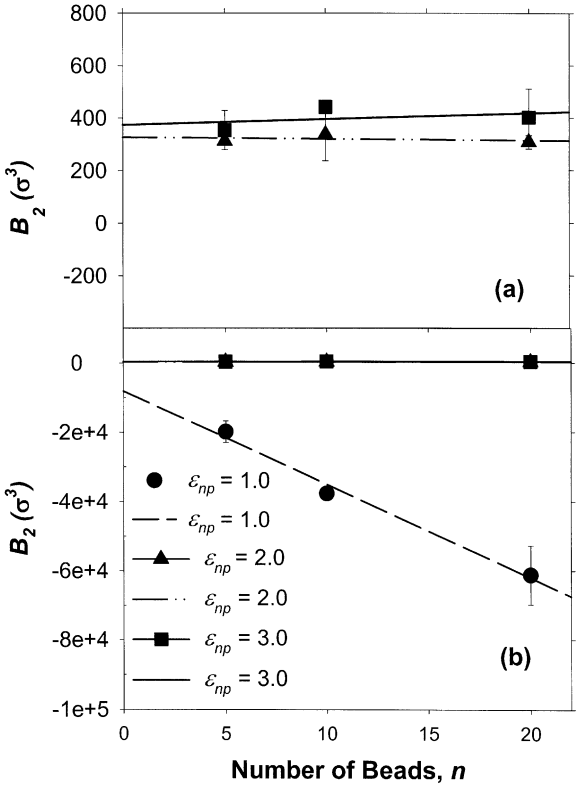

Fig. 7. Second virial coefficient dependence with molecular weight for (a) $\varepsilon_{np} = 2.0$ and 3.0, (b) all ε_{np}. B_2 was calculated from the simulated potential of mean force between nanoparticles in melts of various chain length, n. Lines serve to guide the eye. Error bars were determined from statistical variance between individual simulation runs.

In Fig. 7 B_2 is shown as a function of chain length for $\varepsilon_{np} = 1.0$, 2.0 and 3.0. The effect of molecular weight on the second virial coefficient, and hence the anticipated aggregation/dispersion of nanoparticles, is much less dramatic than the influence of the strength of the polymer–nanoparticle interaction. The tendency to aggregate, as indicated by a negative value of B_2, increases with increasing molecular weight at $\varepsilon_{np} = 1.0$, but the tendency to disperse (positive B_2) is independent of molecular weight for $\varepsilon_{np} = 2.0$ and 3.0.

4. Conclusions and future work

MD simulation studies of matrix-induced interaction between nanoparticles were conducted for model PNPCs where the radius of the nanoparticle, the radius of gyration of the polymer and the statistical segment length of the polymer are comparable. Our simulations reveal that the matrix-induced interaction between nanoparticles in a model PNPC is longer-range than the bare nanoparticle–nanoparticle interaction employed in the simulations and is dependent upon both the molecular weight of the polymer and the strength of the nanoparticle–polymer interaction. For relatively weak nanoparticle–polymer interactions, the polymer matrix promotes aggregation. Here we found that the density of polymer beads between the nanoparticles decreases rapidly for separations less than about three monomer diameters, perhaps reflecting depletion effects due to configurational restrictions (reduced entropy) of polymer chains located between the closely-spaced particles. Increasing the strength of the (attractive) polymer–nanoparticle interaction can overcome polymer matrix driven nanoparticle aggregation, resulting in dispersion of the nanoparticles within the polymer melt. The resultant adsorption of polymer segments on the nanoparticle surface leads to an increase the density of polymer beads between nanoparticles at shorter separations and engenders structure (minima and maxima) in the potential of mean force with a spacing equal to the monomer diameter. The behavior of the nanoparticle second virial coefficient, B_2, confirms that nanoparticle aggregation (attraction) increases with molecular weight for relatively weak polymer–nanoparticle interactions. B_2 was molecular weight independent for systems with strong polymer–nanoparticle interactions. The tendency for dispersion or aggregation of nanoparticles based on

the second virial coefficient was confirmed by simulation of PNPCs containing multiple nanoparticles.

A more comprehensive study of the phase behavior of the model PNPCs studied here as a function of polymer–nanoparticle interactions, particle radii, and polymer molecular weight is currently being conducted. Further study, in conjunction with a detailed analysis of the energetic and entropy contributions to $V_{\text{matrix}}(r)$ as a function of polymer molecular weight and the strength of the polymer–nanoparticle interactions, will help resolve the importance, range and origin of molecular weight and polymer–nanoparticle interaction dependent matrix effects on the phase behavior (aggregation/dispersion) of nanoparticles in PNPCs.

Acknowledgements

Support for this work came from NASA Langley through grant NAG-12319 and the Department of Energy through grant DEFG0301ER45914.

References

[1] Guild F. Quasielastic mechanical properties. In: Paul D, Bucknall C, editors. Polymer blends, vol. 2. New York: John Wiley & Sons; 2000.
[2] McCrum N, Buckley C, Bucknall C. Principles of polymer engineering. New York: Oxford University Press; 1988.
[3] Huber G, Vilgis T, Heinrich G. Universal properties in the dynamical deformation of filled rubbers. J Phys Conds Matter 1996;8:L409–0L412.
[4] Selvan S, Hayakawa T, Masayuki N, Moller M. Block copolymer mediated synthesis of gold quantum dots and novel gold-ply-pyrrole nanocomposites. J Phys Chem B 1999;103(35):7441–8.
[5] Gomoll A, Bellare A, Fitz W, Thornhill T, Scott R, Jemian P, Long G. A nano-composite poly(methyl-methacrylate) bone cement. In: Komarneni S, Parker J, Hahn H, editors. Nanophase and nanocomposite materials III: Materials Research Society Proceedings, vol. 581. Boston (MA, USA): MRS; 2000. p. 399–404.
[6] Mcmanus A, Siegel R, Doremus R, Bizios R. In vitro evaluation of novel polymer/ceramic nanocomposites for orthopedic material applications. Annals Biomedical Eng 2000;28(Suppl. 1):S–15.
[7] Akane O, Kawasumi M, Usuki A, Kojima Y, Kurauchi T, Kamigaito O. Nylon 6–clay hybrid. In: Schaefer D, Mark J, editors. Polymer based molecular composites: Materials Research Society Symposium Proceedings, vol. 171. Boston (MA, USA): MRS; 1990.
[8] Vaia R, Giannelis E. Polymer nanocomposites: status and opportunities. MRS Bulletin 2001;26(5):394–401.
[9] Asakura S, Oosawa F. Interaction between particles suspended in solutions of macromolecules. J Polym Sci 1958;33:183–92.
[10] Asakura S, Oosawa F. On interaction between two bodies immersed in a solution of macromolecules. J Chem Phys 1954;22:1255–6.
[11] Vrij A. Polymers at interfaces and the interactions in colloidal dispersions. Pure Appl Chem 1976;48:471–83.
[12] Gast A, Hall C, Russel W. Polymer-induced phase separations in nonaqueous colloidal suspensions. J Colloid Interface Sci 1983;96(1):251–67.
[13] Lekkerkerker H, Poon W, Pusey P, Stroobants A, Warren P. Phase behaviour of colloid + polymer mixtures. Europhys Lett 1992;20(6):559–64.
[14] Meijer E, Frenkel D. Colloids dispersed in polymer solutions. A computer simulation study. J Chem Physics 1994;100(9):6873–87.
[15] Fuchs M, Schweizer K. Structure of colloid–polymer suspensions. J Phys: Cond Matter 2002;14:R239–0R269.
[16] Fuchs M, Schweizer K. Macromolecular theory of solvation and structure in mixtures of colloids and polymers. Phys Rev E 2001;64:021514.
[17] Starr F, Schroder T, Glotzer S. Effects of nanoscopic filler on the structure and dynamics of a simulated polymer melt and the relationship to ultrathin films. Phys Rev E 2001;64:021802.
[18] Smith, G., Bedrov, D., Li, L., Byutner, O., A molecular dynamics simulation of the viscoelastic properties of polymer nanocomposites. J Chem Phys 2002;117:9478–89.
[19] Vacatello M. Monte Carlo simulations of polymer melts filled with solid nanoparticles. Macromolecules 2001;34:1946–52.
[20] Ginzburg V, Balazs A. Calculating phase diagrams for nanocoomposites: the effect of adding end-functionalized chains to polymer/clay mixtures. Adv Mater 2000;23(12):1805 –1809.
[21] Thompson R, Ginzberg V, Matsen M, Balazs A. Block copolymer-directed assembly of nanoparticles: forming mesoscopically ordered hybrid materials. Macromolecules 2002;35:1060–71.
[22] Ginzburg V, Qiu F, Balazs A. Three-dimensional simulations of diblock copolymer/particle composites. Polymer 2002;43:461–6.
[23] Ginzburg V, Gibbons C, Qiu F, Peng G, Balazs A. Modeling the dynamic behavior of diblock copolymer/particle composites. Macromolecules 2000;33:6140–7.
[24] Balazs A, Ginzburg V, Qui F, Peng G, Jasnow D. Multi-scale model for binary mixtures containing nanoscopic particles. J Phys Chem B 2000;104:3411–22.
[25] Mendez S, Curro J, Pütz M, Bedrov D, Smith G. An integral equation theory for polymer solutions: explicit inclusion of the solvent molecules. J Chem Phys 2001;115(12):5669–75.
[26] Bedrov D, Smith G, Douglas J. Influence of self-assembly on dynamical and viscoelastic properties of telechelic polymer solutions. Europhysics Lett 2002;89(3):384–90.
[27] Palmer B. Direct application of SHAKE to the velocity verlet algorithm. J Comp Phys 1993;104:470–2.
[28] McQuarrie D. Statistical mechanics. New York: Harper & Row; 1976.
[29] Lucretius. A molecular simulation package. Available from: http://www.che.utah.edu/~gdsmith/mdcode/main.html.
[30] Martyna G, Tuckerman M, Tobias D, Klien M. Explicit reversible integrators for extended systems dynamics. Mol Phys 1996;87(5):1117–57.
[31] Torrie G, Valleau J. Nonphysical sampling distributions in Monte Carlo free-energy estimation: umbrella sampling. J Comp Phys 1977;23:187–99.
[32] Frenkel D, Smit B. Understanding molecular simulation from algorithms to applications. New York: Academic Press; 1996.
[33] Ferrenberg A, Swendsen H. Optimized Monte Carlo data analysis. Phys Rev Lett 1989;63(12):1195–8.
[34] Binder K. (editor). Monte-Carlo and molecular dynamics simulations in polymer science. Oxford: New York; 1995.